Response to the reviews of tc-2023-79 "Understanding influence of ocean waves on Arctic sea ice simulation: A modeling study with an atmosphere-ocean-wave-sea ice coupled model" by Chao-Yuan Yang, Jiping Liu, Dake Chen

Responses to comments by Reviewer #1

We would like to thank the reviewer for the helpful comments on the paper.

With the reduction of Arctic sea ice, the expansion of summer sea ice marginal ice zone, and the enhanced moveability of sea ice, understanding influence of ocean waves on Arctic sea ice simulation and the role of floe size on the wave-ice interactions and ice-ocean heat exchange is becoming more important for both research communities from the Arctic sea ice numerical simulation and other related disciplines. This manuscript by Yang et al. investigates the impacts of ocean waves on Arctic sea ice simulation based on a newly-developed atmosphere-ocean-wave-sea ice coupled model. Especially, the contrasting behaviors of floe size, the responses of sea ice to different lateral melting rate formulations, and the sensitivity of sea ice to the simulated wave parameters have been investigated in detail. This is a work worth publishing. However, there are still some confusions that need further revision and clarification. Therefore, I recommend that this paper be considered for publication after minor revisions.

The major point of concern is the simulation effect of oceanic mixed layer. This paper discusses the reshaping process of sea waves on the size of floating ice, as well as the impact of the latter on ice-ocean heat exchange. Then I think the simulation effect of the ocean mixed layer must be discussed, so I suggest adding 1-2 illustrations to compare the simulation results of the depth and heat content of the mixed layer under different mode settings, and discuss on their influence on ice-ocean heat flux.

Response: Thanks for the reviewer's helpful comment. In this revision, we determined

the mixed layer depth (MLD) based on 0.1 degree Celsius difference relative to the surface temperature (e.g., Courtois et al., 2017, their Table 2). The choice of the temperature difference method for MLD determination is due to the calculation of heat content within MLD, which is mainly controlled by the temperature difference between ocean temperature and freezing point. Figure R1-R4 show the monthly-mean of MLD in March and September for all experiments conducted in this study with the same grouping described in Section 3 of the manuscript. In general, as shown in Fig. R1-R4, all experiments exhibit similar evolution of MLD, that is MLD is deeper (up to 150m) in March and shallower (up to 80m) in September. MLD in the open waters is broadly similar across all experiments and MLD near the ice edge (15% ice concentration, black contour in Fig. R1-R4) is shallower (10-30m) relative to other areas. In March, MLDs under ice-covered areas become deeper as lead time increases.

To calculate the heat content within MLD, we used the same approach for the calculation of melting potential in the ROMS model as described in Smith et al. (2010), which is defined as the vertical integral from surface to MLD of the difference between ocean temperature and freezing point. The calculated values of heat content/melting potential have the same unit (W/m^2) and directionality (positive downward) as ice-ocean heat flux, and they represent the "maximum" heat flux that the ice can extract. Figure R5 and R6 show the heat content of MLD and melting potential for Exp-CFSD and Exp-PFSD in March and September. As shown in Fig. R5-R6, Exp-PFSD shows less the melting potential (0-5m) and the heat content within MLD under ice-covered areas compared to Exp-CFSD. This feature is more pronounced in September than in March. Also, heat content in MLD near ice edge of Exp-PFSD reduces more than other ice-covered areas compared to that of Exp-CFSD, suggesting the role of ice-ocean heat flux. Figure R5 and R6 further support the constraint role of limited oceanic energy to ice melting with respect to varied floe-size not only in the surface layer (i.e., melting potential) but also in

the mixed layer. The above analyses and discussions were added in the revised manuscript L625-L646.

Reference:

Courtois, P., Hu, X., Pennelly, C., Spence, P., and Myers, P. G.: Mixed layer depth calculation in deep convection regions in ocean numerical models, Ocean Modelling, 120, 67-78, http://dx.doi.org/10.1016/j.ocemod.2017.10.007, 2017.

Smith, R., Jones, P., Briegleb, B. P., Bryan, F. O., Danabasoglu, G., Dennis, J. M., Dukowicz, J., Eden, C., Fox-Kemper, B., Gent, P., Hecht, M., Jayne, S., Jochum, M., Large, W., Lindsay, K., Maltrud, M., Norton, N., Peacock, S., Vertenstein, M., and Yeager, S.: The Parallel Ocean Program (POP) reference manual: Ocean component of the Community Climate System Model (CCSM), https://opensky.ucar.edu/islandora/object/manuscripts%3A825/, 2010.

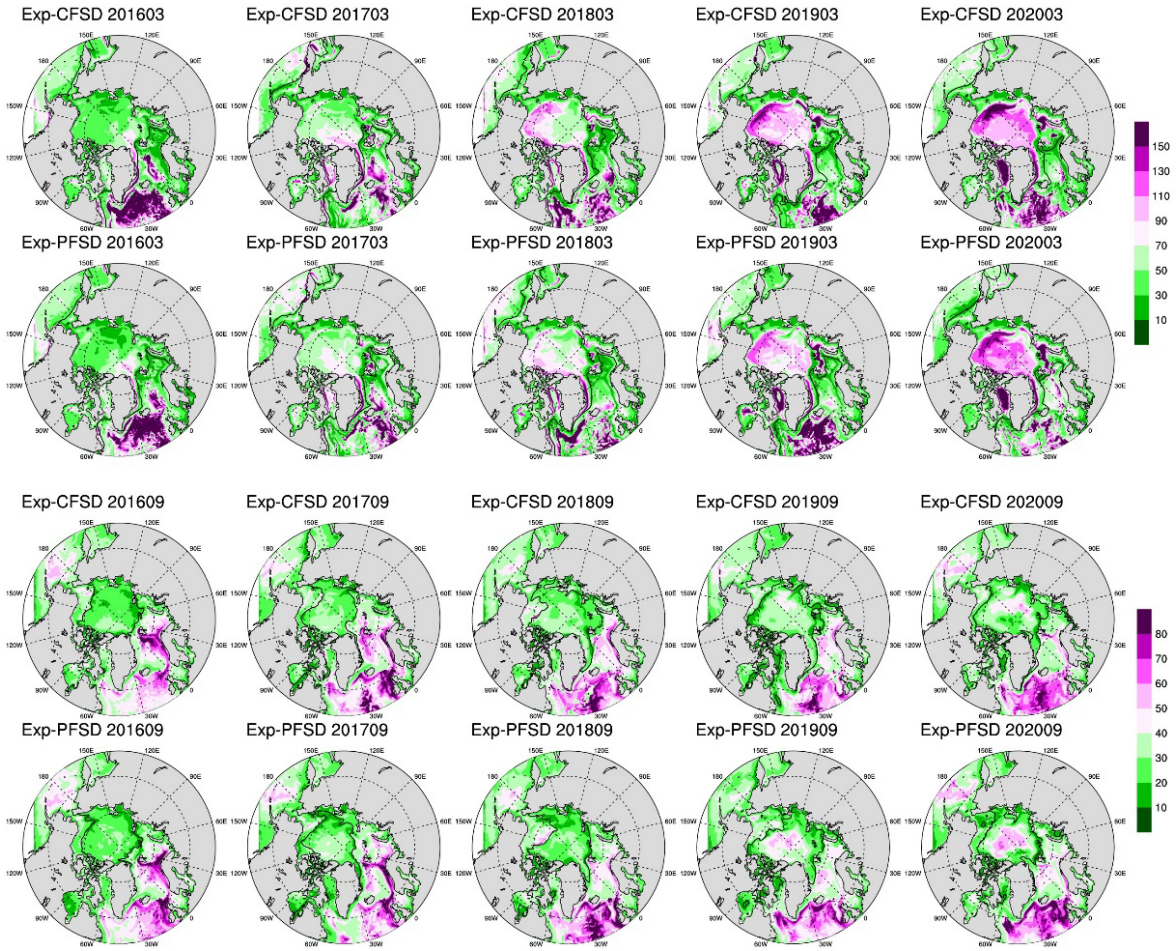

Figure R1 Monthly-mean of MLD in March (top panel) and September (bottom panel) of Exp-CFSD and Exp-PFSD for 2016-2020. Note: black contour represents the averaged location of 15% ice concentration.

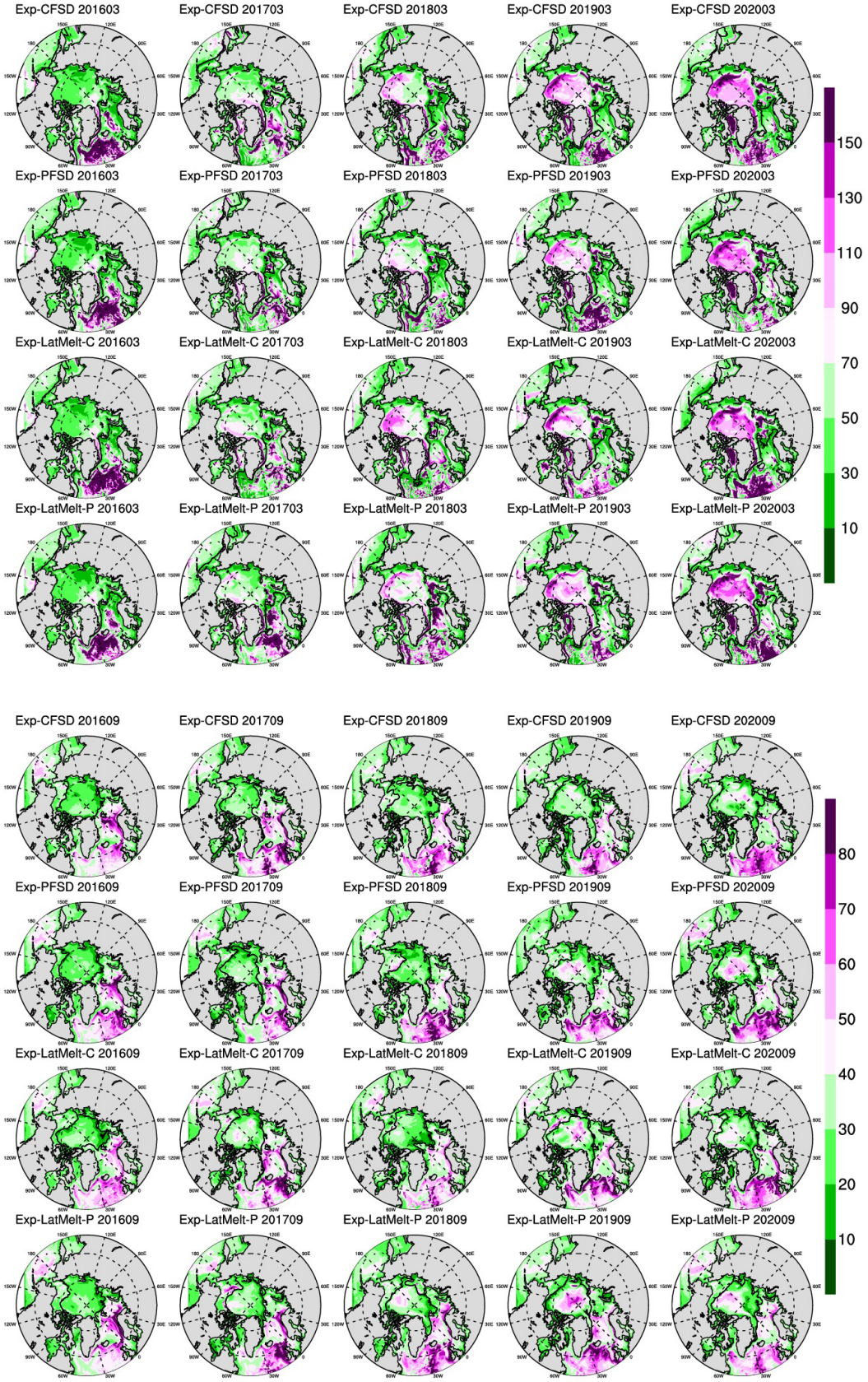

Figure R2 Same as Figure R1 but for Exp-CFSD, Exp-PFSD, Exp-LatMelt-C, and Exp-LatMelt-P.

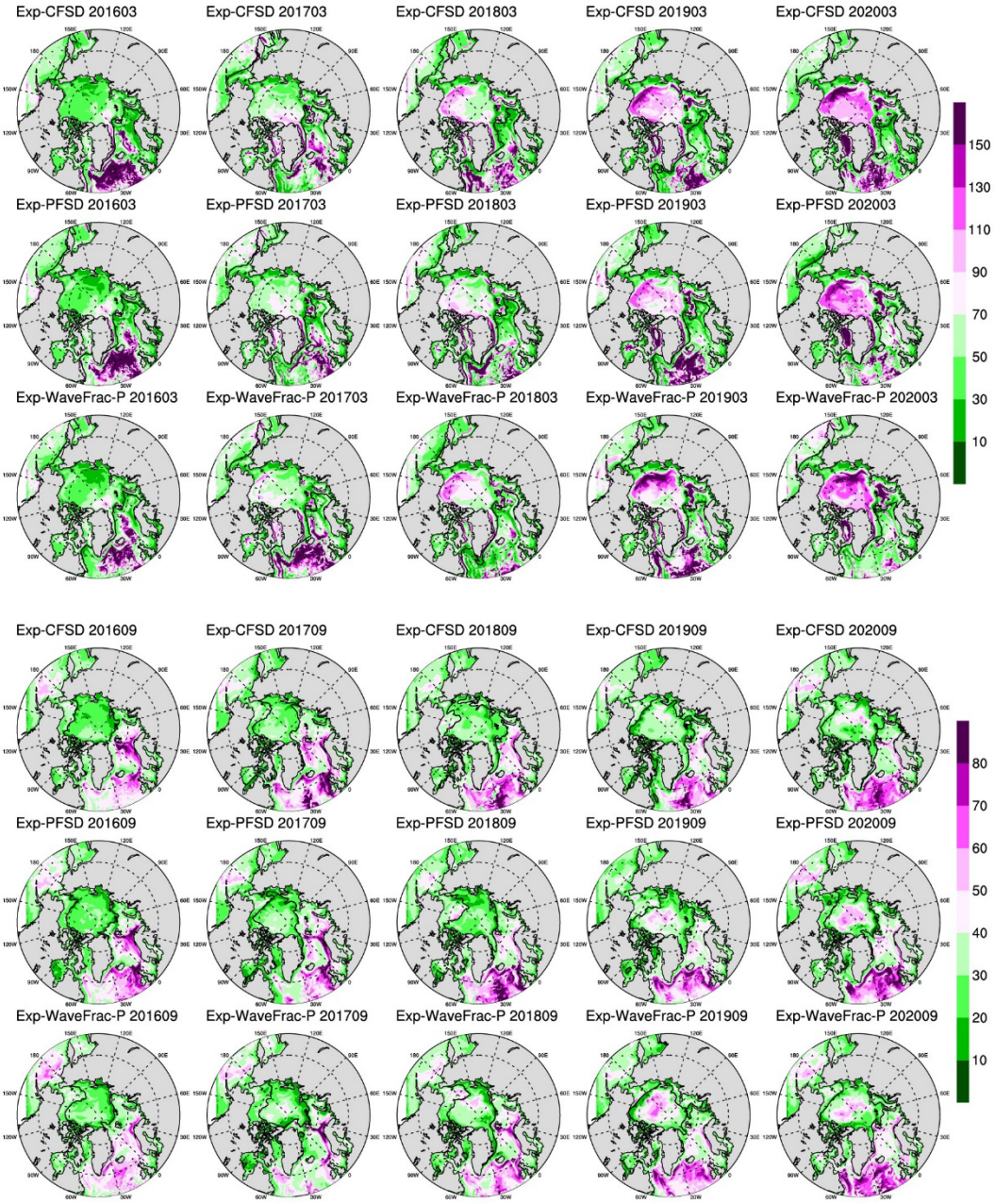

Figure R3 Same as Figure R1 but for Exp-CFSD, Exp-PFSD, and Exp-WaveFrac-P.

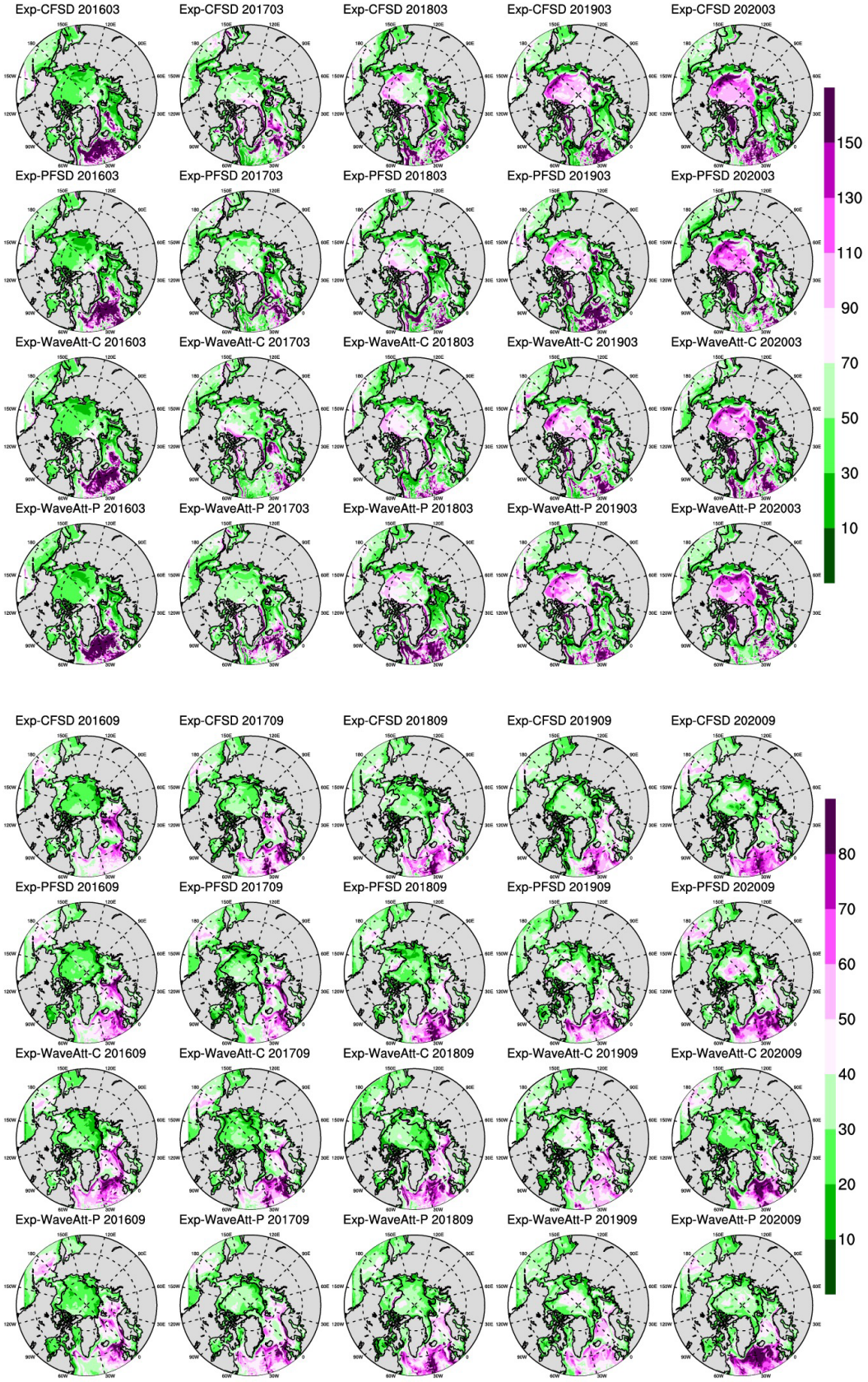

Figure R4 Same as Figure R1 but for Exp-CFSD, Exp-PFSD, Exp-WaveAtt-C, and Exp-WaveAtt-P.

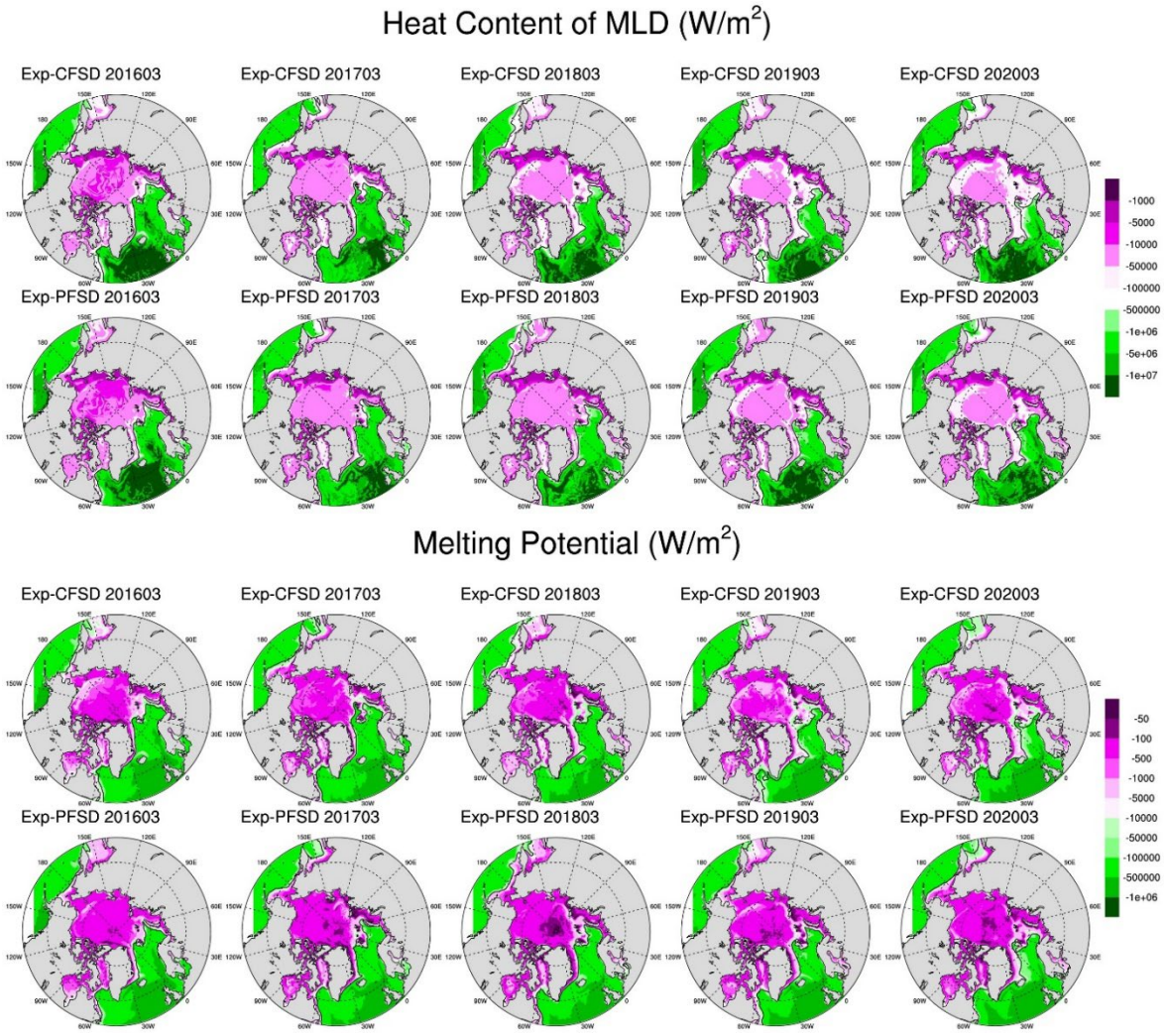

Figure R5 March-averaged heat content of MLD (top panel) and melting potential (bottom panel) of Exp-CFSD and Exp-PFSD for 2016-2020. Note: black contour represents the averaged location of 15% ice concentration.

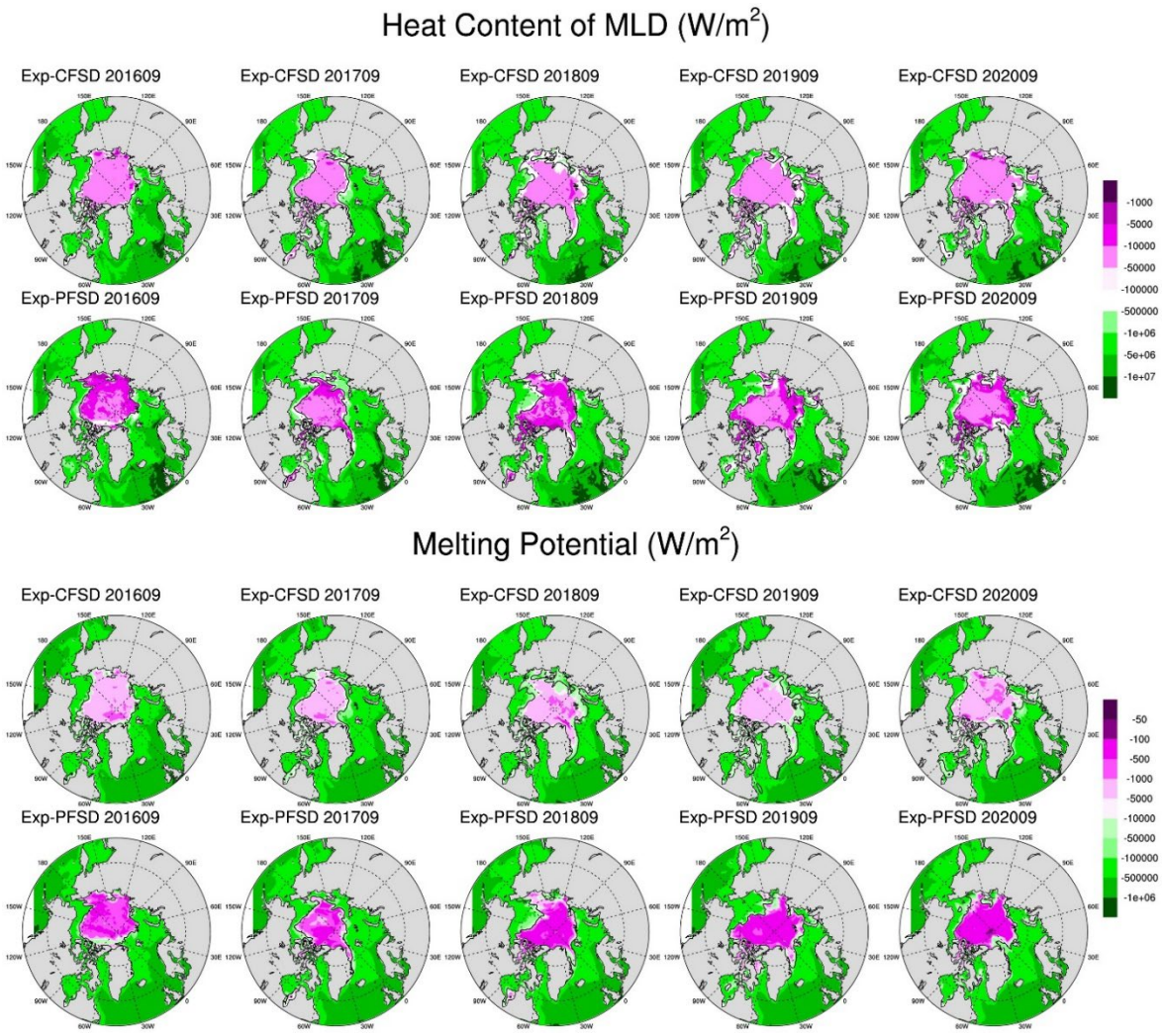

Figure R6 September-averaged heat content of MLD (top panel) and melting potential (bottom panel) of Exp-CFSD and Exp-PFSD for 2016-2020. Note: black contour represents the averaged location of 15% ice concentration.

Other special comments:

Line 56 “the ice-floe melting rate is a result of the interaction between floe size and ocean circulation”: Why the floe size interacts with the ocean circulation is not clear here, what scale of ocean circulation is, and why it affects the ice-ocean heat flux and ice melt rate?

Response: Horvat et al. (2016) set up idealized experiments based on MITgcm with different total numbers of ice floe with the same size uniformly spaced in a 75*75 km

domain, these experiments have the same initial total ice coverage (49.92% of the domain) and ice volume, and ice momentum equation is disabled. At the early stage of simulation, relatively cold and fresh water is formed in the ice-covered areas and leads to density gradient between ice-covered and ice-free regions, and then geostrophic surface currents along the floe edge. Within several days of simulation, baroclinic instabilities appear along the density gradient, mix ocean energy from ice-free areas (where have net incoming heat flux from the atmosphere by design) to under-floe areas, and finally lead to enhanced ice melting. The enhancement of ice melting rate is increasing with the number of floes (i.e., as floe size decreases). Different from Horvat et al. (2016), who only investigated thermodynamics melt of ice floes, Gupta and Thompson (2022) further consider both mechanical and thermodynamics effects on ice floes and also shows the ice melting rate is related to floe size. In this revision, we modified the text to better reflect the processes described above and now it reads as "Some studies also show that the ice-floe melting rate is associated with horizontal mixing of oceanic heat across ice floe edge between open water and under-floe ocean by oceanic eddies, in particular sub-mesoscale eddies, and the strength of this effect depends on floe size (Gupta and Thompson, 2022; Horvat et al., 2016)." in the revised manuscript L55-L58.

Line 62 "Previous studies showed that intense storms like "Great Arctic Cyclone" of 2012 (Simmonds and Rudeva, 2012) and strong summer cyclone in 2016 contribute to the anomalously low sea ice extent in 2012 and 2016": This can only be said to be a partial contribution, as even without great cyclones, there will be an extremely low Arctic sea ice extent in the summer of 2012.

Response: Thanks for the reviewer's comment. We changed this sentence to "Previous studies suggested that intense storms like "Great Arctic Cyclone" of 2012 (Simmonds and

Rudeva, 2012) and strong summer cyclone in 2016 could be one of contributors to the anomalously low sea ice extent in 2012 and 2016…" in the revised manuscript L64-L66.

Line 96 "a full representation of sea ice responses under the interactions across atmosphere, ocean, wave, and sea ice": Actually, waves are a part of the ocean.

Response: Thanks for the reviewer's suggestion. We modified the text to "… a full representation of sea ice responses to the evolving states of atmosphere, ocean, and wave based on explicit model physics as well as feedbacks from sea ice to them" in the revised manuscript L99-L101.

frazil ice formation: the frazil ice is very discrete, how does it affect the air-ocean heat flux?

Response: We follow the nomenclature in the documentation of Sea Ice Model Intercomparison Project (Notz et al., 2016, Append. E), which defines sea ice mass change through ice growth in supercooled open water (a.k.a. frazil ice formation) as one of the sea ice mass budget terms. In this study, frazil ice formation is equivalent to any newly-formed ice mass by supercooled water in the CICE model.

Reference:

Notz, D., Jahn, A., Holland, M., Hunke, E., Massonnet, F., Stroeve, J., Tremblay, B., and Vancoppenolle, M.: The CMIP6 Sea-Ice Model Intercomparison Project (SIMIP): understanding sea ice through climate-model simulations, Geosci. Model Dev., 9, 3427–3446, https://doi.org/10.5194/gmd-9-3427-2016, 2016.

The floe welding parameter: How to consider the seasonal changes in the welding coefficient

of sea ice, especially during the freeze-thaw transition season, whether it will be affected by ice temperature and thickness? If the seasonal variation of welding coefficient is considered, how will it affect the simulation results ?

Response: As described in Roach et al. (2018), the floe welding process only occurs in the freezing condition. In this study, the freezing condition of each cell is determined by the net ice mass increase based on sea ice mass budget terms excluding the dynamics term. Then, the floe welding parameter acts like a step function once the freezing condition is met, and its value changes from 0 to the prescribed value (section 3 in the manuscript). In addition to the step function-like behavior of the floe welding parameter, sea ice concentration also contributes to seasonal changes of the floe welding process from the formulation perspective. The floe welding process is parameterized as (Roach et al., 2018),

$$\frac{\partial N}{\partial t} = -\frac{\kappa}{2} C^2$$

where N is floe number density, κ is the floe welding parameter, and C is sea ice concentration, and the changes in N is proportional to the square of C. Combined the step-change of the floe welding parameter between the freeze-thaw transition and the seasonal signal of ice concentration, the seasonal changes in the floe welding process are considered in this study. However, whether the floe welding parameter itself is a function of other variables (e.g., ice thickness, ice temperature) is still an open question due to limited field observations and laboratory experiments. The duration of contact between floes, the heat loss from the floes, or the overlap area between floes might be also important for the floe welding process (e.g., Manucharyan and Montemuro, 2022; Shen and Ackley, 1991). In this revision, we added more descriptions for the freeze-thaw transition of the welding parameter in Section 3 of the revised manuscript L278-L282.

Reference:

Manucharyan, G. E., and Montemuro, B. P.: SubZero: A sea ice model with an explicit representation of the floe life cycle. Journal of Advances in Modeling Earth Systems, 14, e2022MS003247. https://doi.org/10.1029/2022MS003247, 2022.

Roach, L. A., Smith, M. M., and Dean, S. M.: Quantifying growth of pancake sea ice floes using images from drifting buoys. Journal of Geophysical Research: Oceans, 123, 2851–2866. https://doi.org/10.1002/2017JC013693, 2018.

Shen, H. H., and Ackley, S. F.: A one-dimensional model for wave-induced ice-floe collisions. Annals of Glaciology, 15, 87–95. https://doi.org/10.1017/s0260305500009587, 1991.

Response to comments by Reviewer #2

We would like to thank the reviewer for the helpful comments on the paper.

This study quantifies the effect of ocean waves on sea ice simulation in the arctic based on a coupled model framework built by the authors. Authors focus on the floe size and thickness distribution (FSTD) with the effect of the ocean waves embedded. This study demonstrates that involving wave-related process can have an impact on sea ice, proving the importance of oceanic wave on sea ice modeling in the coupled model.

Overall, the model development work in this study has a significant value on the coupled modeling system. The result in this study offers more insights on the interaction between the atmosphere, ocean, and sea ice in the arctic. The whole manuscript is well-written in general, and I recommend an acceptance after some minor revisions.

Major points:

In this study, the authors divide the model domain into 3 sub-regions, while it lacks conclusions

that related to geographically-specified features. I understand that the model development in this study has a good application for all these three regions, and it can distinguish the different wave-sea ice interactions in these regions. But authors should elaborate more on how the regional features derives the conclusion that are widely-applicable for the pan-arctic.

Response:

Thanks for the reviewer's constructive comment. In this revision, we added additional text and an additional figure to better illustrate geographically-specified features of 3 sub-regions. In the revised manuscript L435-L447, now it reads "… the strengthened vertical mixing brings warmer water of the subsurface upward and maintains/increases the melting potential in the subregions. Figure 8d-f also show that the warmer signal in the upper ocean (at least to 60m depth) of Exp-PFSD persists after July, 2018 in the ATL region while the LK and BCE regions show seasonal oscillation of ocean temperature in the upper ocean for the entire simulation. Combined with the regional SIA shown in Figure 7d-f, seasonal fully ice-covered states in the LK and BCE regions force the upper ocean to restore to certain states (i.e., near freezing point under sea ice, near zero melting potential shown in Fig. 7k-l) for both Exp-CFSD, and Exp-PFSD, which might mitigate the effects of ocean wave activities and other processes on the upper ocean. Figure 9(R7) shows the difference of dynamical and thermal mass change between Exp-PFSD and Exp-CFSD. With less restoring effect by sea ice on the upper ocean in the ATL regions, the difference of thermally-induced mass change between Exp-PFSD and Exp-CFSD shows a larger variation once the upper ocean difference starts to persist after July, 2018 (Fig. 8d, 9d) while the variations in the LK and BCE regions remain relatively unchanged for the entire simulation (Fig. 9e-f)."

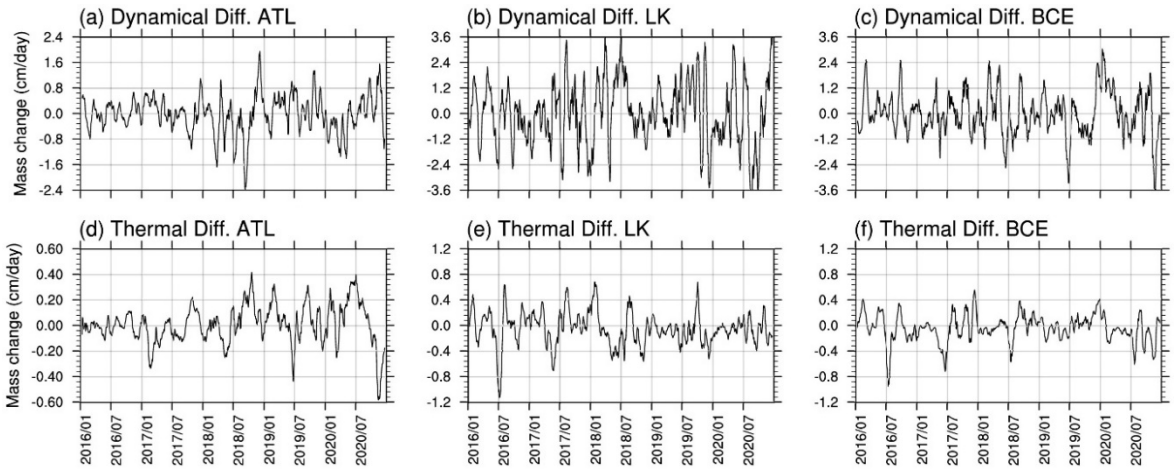

Figure R7 Time-series of the difference of (a-c) dynamical mass change and (d-f) thermal mass change between Exp-PFSD and Exp-CFSD in the ATL, LK, and BCE regions.

Minor points

Line 238: Please specify that if the atmosphere, ocean, and sea ice model are using the same model grid.

Response: Thanks for the reviewer's comment. We changed the sentence to "The WRF, ROMS, SWAN, and CICE models use the same model grid with 320 (440) x- (y-) grid points and ~24km horizontal resolution (Fig. 1)" in the revised manuscript L242-L243.

Line 248: The model configuration of a higher model top is kind of confusing to me. Does it only matter on the atmospheric circulation modeling? Or it has some effect on the better coupling between the atmosphere and ocean/sea ice?

Response: Cassano et al. (2011) showed that a higher model top can reduce the bias in the simulated sea level pressure (SLP) based on the standalone WRF model. Without an elevated model top, and the circulation biases exhibit not only in SLP but also enhance with height. They suggested that this top-down bias in the circulation is associated with

the model-top boundary treatment, which is also shown in other modeling studies (ARCSyM, Lynch and Cullather, 2000; HadAM3, Scaife et al., 2005). In our preliminary multiyear simulations with our coupled model before conducting this study, the higher model top can lead to better simulated ice mass distribution, which might be able to interpreted as better coupling between the atmosphere and sea-ice.

Reference:

Cassano, J. J., Higgins, M. E., and Seefeldt, M. W.: Performance of the Weather Research and Forecasting Model for Month-Long Pan-Arctic Simulations. Monthly Weather Review, 139, 11, 3469-3488, https://doi.org/10.1175/MWR-D-10-05065.1, 2011.

Lynch, A. H., and Cullather, R. I.: Investigation of boundary forcing sensitivities in a regional climate model. J. Geophys. Res., 105, 26603–26617, 2000.

Scaife, A. A., Knight, J. R., Vallis, G. K., and Folland, C. F.: A stratospheric influence on the winter NAO and North Atlantic surface climate. Geophys. Res. Lett., 32, L18715, doi:10.1029/2005GL023226, 2005.

Figure 9 make sure the naming of sub-figures correctly follows the rule of TC.

Response: Thanks for the reviewer's suggestion. We re-plotted all figures using sub-indexing for the naming in this revision as shown in Figure R8-R10.

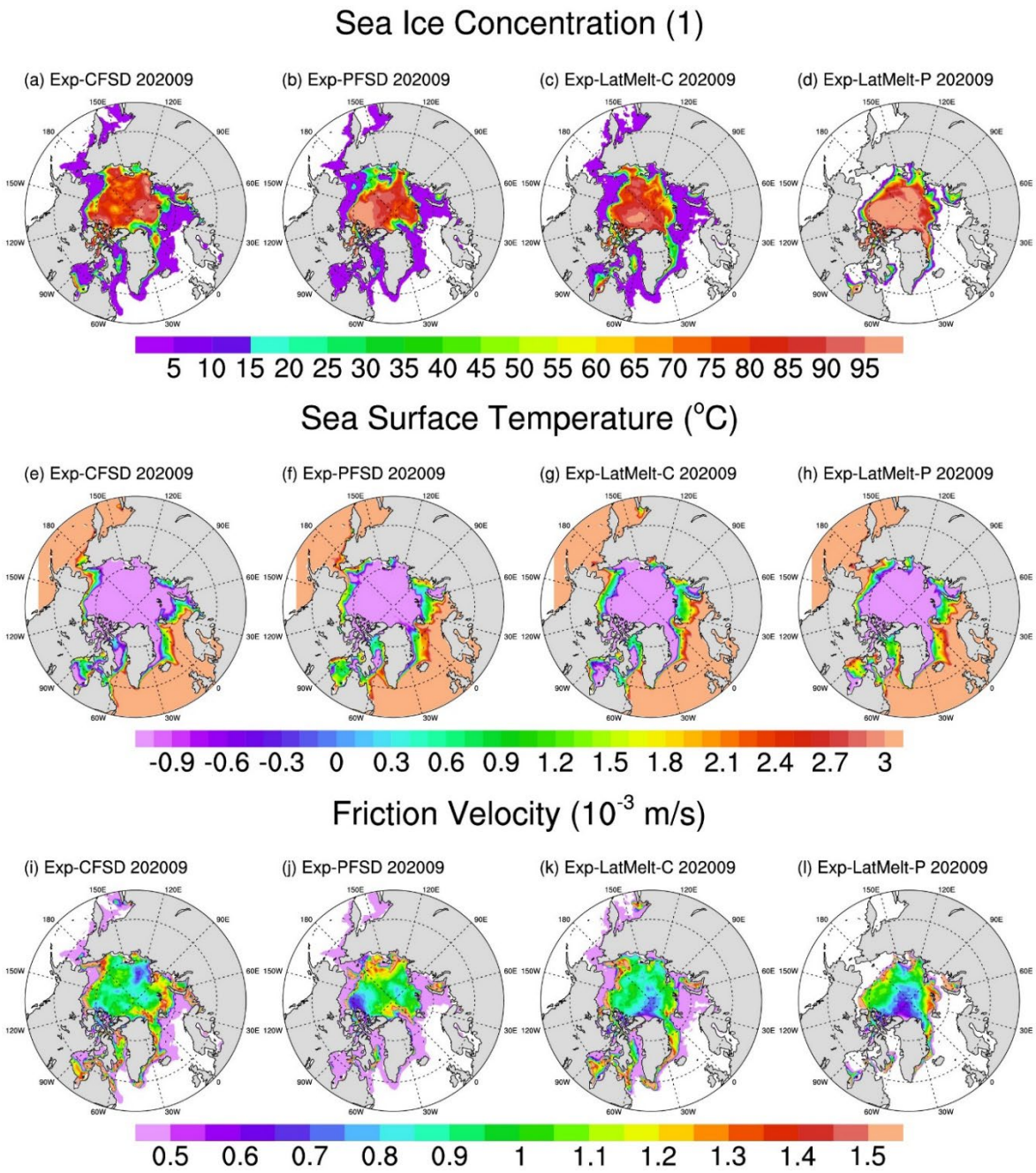

Figure R8 The monthly-mean of (a-d) sea ice concentration, (e-h) sea surface temperature, and (i-l) friction velocity in September, 2020 for Exp-CFSD, Exp-PFSD, Exp-LatMelt-C, and Exp-LatMelt-P.

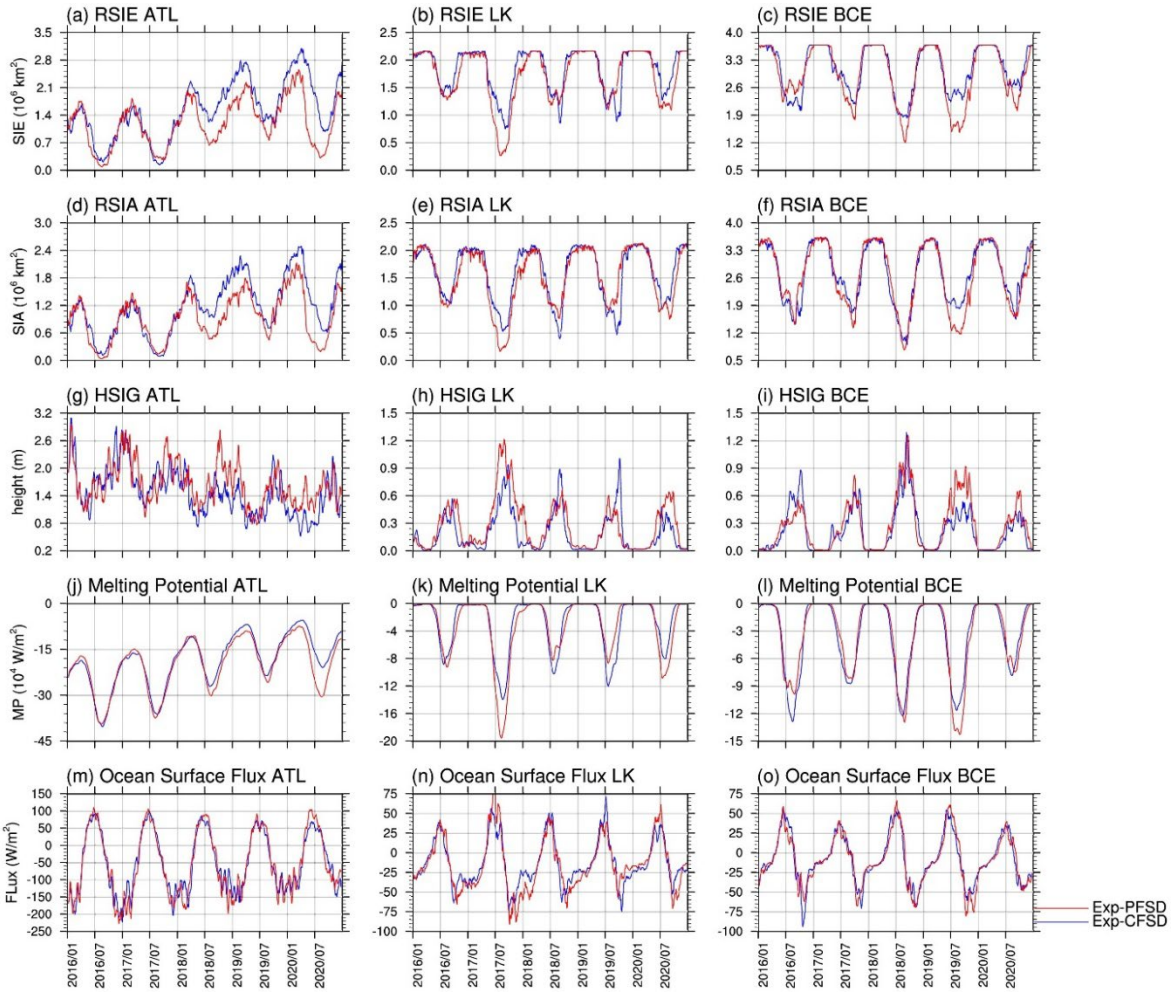

Figure R9 Time-series of (a-c) ice extent, (d-f) ice area, (g-i) significant wave height, (j-l) melting potential, and (m-o) heat flux at the ocean surface in ATL, LK, and BCE regions for Exp-CFSD (blue line) and Exp-PFSD (red line). Note: significant wave height, melting potential, and heat flux at the ocean surface are region-averaged and 15-day running-averaged values.

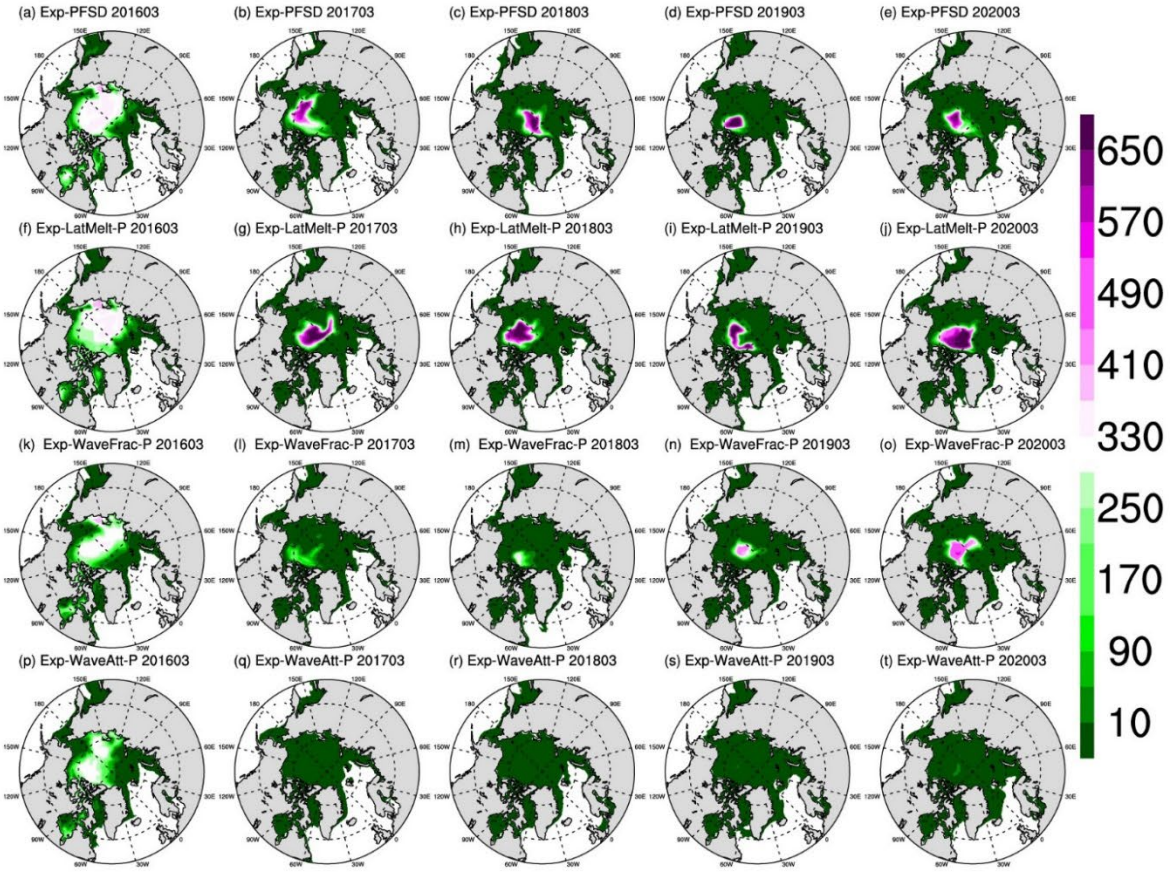
(a) Exp-PFSD 201603
(b) Exp-PFSD 201703
(c) Exp-PFSD 201803
(d) Exp-PFSD 201903
(e) Exp-PFSD 202003
(f) Exp-LatMelt-P 201603
(g) Exp-LatMelt-P 201703
(h) Exp-LatMelt-P 201803
(i) Exp-LatMelt-P 201903
(j) Exp-LatMelt-P 202003
(k) Exp-WaveFrac-P 201603
(l) Exp-WaveFrac-P 201703
(m) Exp-WaveFrac-P 201803
(n) Exp-WaveFrac-P 201903
(o) Exp-WaveFrac-P 202003
(p) Exp-WaveAtt-P 201603
(q) Exp-WaveAtt-P 201703
(r) Exp-WaveAtt-P 201803
(s) Exp-WaveAtt-P 201903
(t) Exp-WaveAtt-P 202003
650
570
490
410
330
250
170
90
10

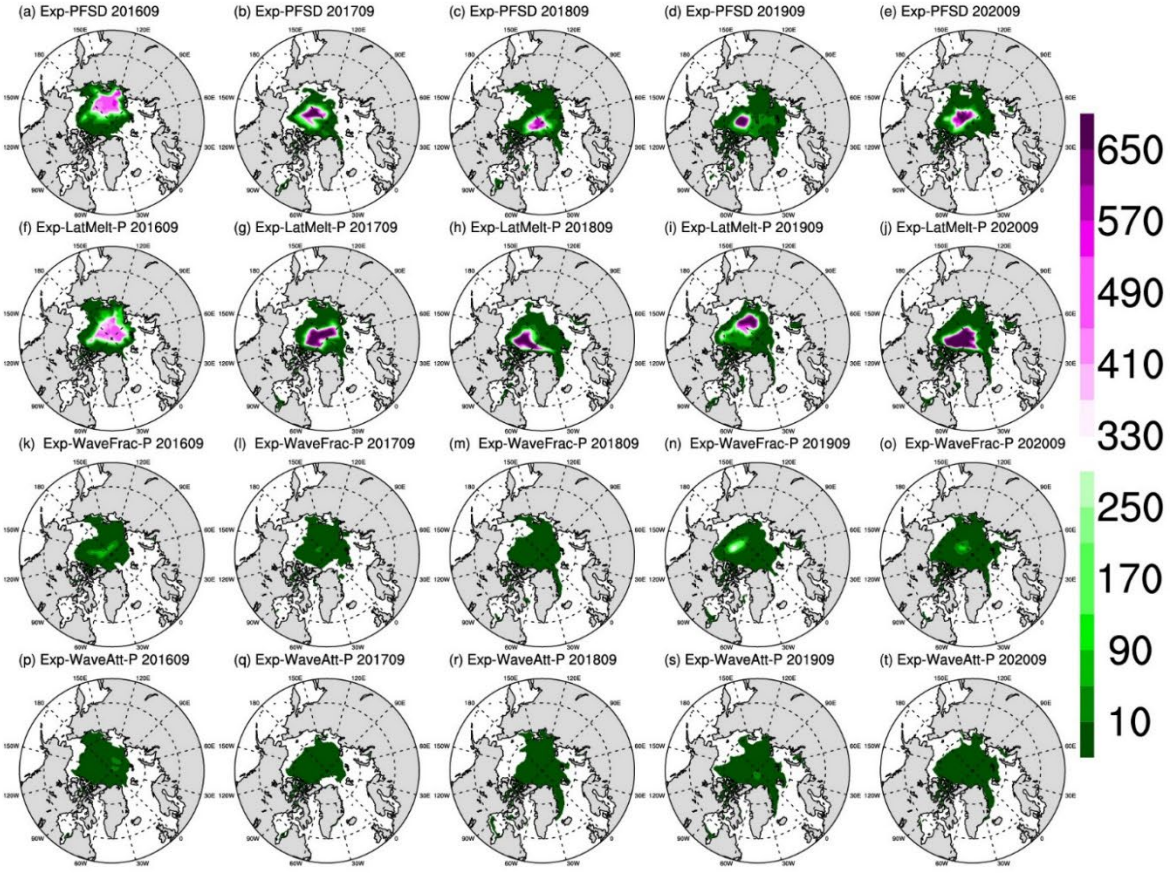
(a) Exp-PFSD 201609
(b) Exp-PFSD 201709
(c) Exp-PFSD 201809
(d) Exp-PFSD 201909
(e) Exp-PFSD 202009
(f) Exp-LatMelt-P 201609
(g) Exp-LatMelt-P 201709
(h) Exp-LatMelt-P 201809
(i) Exp-LatMelt-P 201909
(j) Exp-LatMelt-P 202009
(k) Exp-WaveFrac-P 201609
(l) Exp-WaveFrac-P 201709
(m) Exp-WaveFrac-P 201809
(n) Exp-WaveFrac-P 201909
(o) Exp-WaveFrac-P 202009
(p) Exp-WaveAtt-P 201609
(q) Exp-WaveAtt-P 201709
(r) Exp-WaveAtt-P 201809
(s) Exp-WaveAtt-P 201909
(t) Exp-WaveAtt-P 202009
650
570
490
410
330
250
170
90
10

Figure R10 The spatial distribution of the representative floe radius in March (upper panel) and September (bottom panel) of (a-e) Exp-PFSD, (f-j) Exp-LatMelt-P, (k-o) Exp-WaveFrac-P, and (p-t) Exp-WaveAtt-P for 2016-2020. Note: cells with less than 15% ice concentration are treated as missing values.